Evolution and extinction of the giant rhinoceros *Elasmotherium sibiricum* sheds light on late Quaternary megafaunal extinctions

Pavel Kosintsev[1], Kieren J. Mitchell[2], Thibaut Devièse[3], Johannes van der Plicht[4,5], Margot Kuitems[4,5], Ekaterina Petrova[6], Alexei Tikhonov[6], Thomas Higham[3], Daniel Comeskey[3], Chris Turney[7], Alan Cooper[2], Thijs van Kolfschoten[5], Anthony J Stuart[8], Adrian M Lister[9*].

[1] Institute of Plant and Animal Ecology, Ural Branch, Russian Academy of Sciences, 8 Marta St. 202, Yekaterinburg 620144, Russia

[2] Australian Centre for Ancient DNA, School of Biological Sciences, University of Adelaide, North Terrace Campus, South Australia 5005, Australia

[3]Oxford Radiocarbon Accelerator Unit, University of Oxford, 1-2 South Parks Road, Oxford, OX1 3TG, UK

[4] Center for Isotope Research, Groningen University, Groningen, The Netherlands

[5] Faculty of Archaeology, Leiden University, P.O. Box 9514, 2300 RA Leiden, The Netherlands

[6] Zoological Institute, Russian Academy of Sciences, 1 Universitetskaya Naberezhnaya, St. Petersburg, 199034, Russia

[7] Palaeontology, Geobiology and Earth Archives Research Centre, and Climate Change Research Centre, School of Biological, Earth, and Environmental Sciences, University of New South Wales, Sydney, Australia.

[8] Department of Biosciences, Durham University, South Road, Durham DH1 3LE, UK

[9] Department of Earth Sciences, Natural History Museum, London SW7 5BD, UK

* Author for correspondence: A.Lister@nhm.ac.uk

Understanding extinction events requires an unbiased record of the chronology and ecology of victims and survivors. The rhinoceros *Elasmotherium sibiricum*, known as the 'Siberian unicorn', was believed to have gone extinct around 200 ka, well before the Late Quaternary megafaunal extinction event. However, no absolute dating, genetic analysis, or quantitative ecological assessment of this species has been undertaken. Here we show, by AMS radiocarbon dating of 23 individuals, including cross-validation by compound specific analysis, that *E. sibiricum* survived in Eastern Europe and Central Asia until at least 39 ka BP, corroborating a wave of megafaunal turnover prior to the Last Glacial Maximum in Eurasia, in addition to the better-known Late-glacial event. Stable isotope data indicate a dry steppe niche for *E. sibiricum* and, together with morphology, a highly specialised diet that likely contributed to its extinction. We further demonstrate, with DNA sequence data, a very deep phylogenetic split between the subfamilies Elasmotheriinae and Rhinocerotinae that includes all the living rhinos, settling a debate based on fossil evidence and confirming that the two lineages had diverged by the Eocene. As the last surviving member of the Elasmotheriinae, the demise of the 'Siberian unicorn' marked the extinction of this subfamily.

The rhinoceros family (Rhinocerotidae) was formerly much more diverse than it is today, with some 250 named species[1] of which only five survive. During the Miocene (ca. 23-5 Ma), rhinos were a dominant part of the large mammal fauna in Africa, Eurasia, and North America. Phylogenetic analysis of fossil species has resolved two main lineages: the Rhinocerotinae, which includes all living species and the recently-extinct woolly rhinoceros (*Coelodonta antiquitatis*), and the extinct Elasmotheriinae[2]. Based on morphological diagnoses of early remains, the two subfamilies are thought to have diverged very early in rhinoceros evolution, by at latest 35 Ma[2,3]. The Elasmotheriinae subsequently gave rise to some 20 genera, of which only *Elasmotherium* survived the Miocene, with *E. sibiricum* its last surviving member, although some authors have separated *Elasmotherium* from other members of the group and place it within Rhinocerotinae[4,5]. A spectacular megafaunal species of Eurasia, at ca. 3.5 tonnes, *E. sibiricum* was the largest Quaternary rhinoceros. *E. sibiricum* was also remarkable in its anatomy: relatively slender limbs indicating adaptation for running, despite its mass[6]; absence of incisors and canines; and – uniquely among rhinos – continuously-growing cheek-teeth with distinctive, highly convoluted enamel plates. The presence of a massive single horn in *Elasmotherium* has been inferred from the bony protuberance on the frontal bone of the skull which implies a horn base much larger than in any other rhino, living or extinct; hence the informal name 'Siberian unicorn' (Fig. 1). The known geographical ranges of both *E. sibiricum* and related (in some cases possibly synonymous) *Elasmotherium* species were very limited, with most confirmed records from Kazakhstan, western and central Russia, Ukraine, Azerbaijan, Uzbekistan, as well as isolated finds (referred to *E. caucasicum*) from Mongolia and China[2,7,8] (Fig. 2). *E. sibiricum* was thought to have become extinct by 200,000 years ago, although recent, unconfirmed reports suggested that it might have persisted into the Late Pleistocene[7,9]. Its ecological niche has been a matter of speculation, from grazing on dry steppes to foraging for roots in damp riverine environments[7].

Results

Direct dating of unambiguously identified remains is an essential prerequisite for determining the extinction chronology of late Quaternary megafauna[10]. Of a total of 25 *Elasmotherium sibiricum* bone samples analysed in the present study, 23 contained sufficient collagen for radiocarbon dating (Supplementary Table 1, Fig. 3). All samples were first dated by Accelerator Mass Spectrometry (AMS) either at the Groningen Centre for Isotope Research (CIO), Netherlands (lab code GrA) or at the Oxford Radiocarbon Accelerator Unit (ORAU), UK (lab code OxA) using the routine procedures (See Methods). All nine samples yielding dates younger than 35,000 radiocarbon years were then cross-dated by the other laboratory (Supplementary Table 1), and the results were compared using a chi-squared test (Supplementary Table 8). In five of nine cases, the pairs of dates were not statistically distinguishable. For the other four paired samples, however, there was a discrepancy between the dates obtained in the two laboratories. In two cases the dates obtained in Oxford were older than those obtained in Groningen, in the other two cases the opposite was the case. These differences are likely due to contamination which could not be totally removed using standard methods of collagen purification. For two samples (IPAE 897/123 and ZIN 36330), the difference between the dates obtained by the two laboratories was ~10,000 years. It was therefore decided to undertake further dating of all nine samples using the single amino acid radiocarbon method developed at the ORAU[11]. This method involves the separation of the underivatised amino acids from hydrolysed bone collagen using preparative High Performance Liquid Chromatography (Prep-

HPLC), isolating the amino acid hydroxyproline for AMS measurement. This pretreatment approach (coded 'HYP') is the most efficient available technique to remove contaminants including, but not limited to, conservation materials (with the exception of collagen-based glue). All of the chronometric data from ORAU is reported in Supplementary Table 7. Chi-squared tests showed that in four of the cases, the dates obtained on ultrafiltered collagen and hydroxyproline are not statistically distinguishable (Supplementary Table 8), indicating that all the contaminant had been removed by the AF/AF* treatment (see Methods). In the other five cases, the dates obtained on hydroxyproline are older than those obtained on collagen both in Groningen and Oxford. For these five samples, we suspect that some contaminant had remained in the collagen (possibly crosslinked to it) but was removed by hydrolysing the collagen and isolating hydroxyproline. Similar observations have been made on a range of contaminated Palaeolithic bone samples (see, for example, refs. [12–16]). Ages obtained on hydroxyproline were therefore retained over those obtained from bulk collagen on these nine samples. In the final dataset of conventional radiocarbon ages (CRA), 19 are finite dates and 5 are beyond the radiocarbon limit. The five youngest ages are all corroborated by HYP. The 19 finite dates were then calibrated against the IntCal13 dataset[17] using OxCal version 4.3[18] (Supplementary Fig. 2), and were incorporated within a single Phase model in OxCal v.4.3 (Supplementary Table 9). We used a General outlier model (prior probability set at 0.05)[19] to explore the degree to which likelihoods were outlying. Using IntCal13, the calibrated 95.4% confidence intervals for the finite ages range in an overlapping series from 50-44.76 to 38.97-36.52 cal ka BP (Fig. 3, Supplementary Fig. 2). The end boundary in the model provides an estimate of the last appearance of *Elasmotherium* at 38.48-35.06 cal ka BP (at 95.4% probability). Our data demonstrate the late Quaternary extinction of *E. sibiricum*, and imply an extinction before the Last Glacial Maximum. With 23 dates this conclusion is provisional, but it is supported by the lack of any known remains in dated post-LGM contexts[20,21].

Six bone samples were subjected to ancient DNA analysis and all yielded usable DNA data, although molecular preservation varied markedly (Supplementary Table 2). We were able to reconstruct a high-quality mitochondrial genome sequence for the best-preserved specimen – IPAE915/2804 (GenBank accession: MH937513) – with a mean read-depth of 116.1×, which covered 99.3% of the modern white rhinoceros reference (*Ceratotherium simum,* NC_001808). It is notable that IPAE915/2804, from Tobolsk (latitude ~58°), is the most northerly of our samples (Fig. 2), possibly accounting for its better DNA preservation. Despite poorer preservation in the other samples – as low as 0.8× depth for 2388/1 – all sequences were very similar to IPAE915/2804 (≥99.7% identical at unambiguously called nucleotide sites).

Phylogenetic analyses including the IPAE915/2804 consensus sequence strongly suggest that *Elasmotherium* is sister-taxon to Rhinocerotinae (Fig. 4; Maximum Likelihood Bootstrap, MLB = 99%, Bayesian Posterior Probability, BPP = 1.0). Relationships among perissodactyls were otherwise concordant with the results of past molecular studies[22,23], although the position of the root of Rhinocerotinae remains poorly resolved.

Our molecular dating analyses suggest that the divergence between *Elasmotherium* and the Rhinocerotinae occurred around 47.3 Ma (95% Highest Posterior Density, HPD = 41.9 – 53.2 Ma). The primary divergence within crown Rhinocerotinae (the split between *Diceros*+*Ceratotherium* and the remaining taxa) occurred 30.8 Ma (95% HPD = 26.5 – 35.3 Ma), while the divergence of Rhinocerotoidea from Tapiroidea occurred 57.5 Ma (95% HPD = 52.6 – 62.8 Ma). Highest Posterior

Densities (HPDs) for node ages estimated in the present study overlapped with those of comparable nodes in previously published studies[23,24]. However, our mean age estimates for nodes deeper in the tree (i.e. crown ages of Perissodactyla and Ceratomorpha) were slightly older than those in previously published studies, as our conservative node age constraints allowed for the possibility that perissodactyl diversification began during the Palaeocene (see Supplementary Information).

For stable isotope analysis, C:N ratios of all samples were within acceptable range (Supplementary Table 6), with the exception of sample IPAE 420-111 which is just outside the range and is excluded from further discussion. The *Elasmotherium* δ^{13}C values (n=22) range from -21.5‰ to -16.3‰ with a mean of -18.1 ±0.3 ‰. The δ^{15}N values (n=21) range from +6.5‰ to +12.8‰ with a mean of +9.4 ±0.3 ‰ (Fig. 5; Supplementary Table 6). The range of stable isotope values might partly be due to geographic or temporal variation, although no trend through time or a correlation with latitude is observed in the data (Supplementary Fig. 1). However, the *Elasmotherium* δ^{13}C and δ^{15}N values clearly differ from those of other fossil Rhinocerotidae from Eurasia (Fig. 5). The majority of *E. sibiricum* individuals are relatively higher in both δ^{13}C and δ^{15}N than narrow-nosed and/or Merck's rhinoceros (*Stephanorhinus hemitoechus/kirchbergensis*) from the Middle Pleistocene of Schöningen, Germany. Most of our samples are also enriched in both δ^{13}C and δ^{15}N than woolly rhinoceros (*Coelodonta antiquitatis*) from within the temporal and geographical range of the *Elasmotherium* material*.* Conversely, *E. sibiricum* overlaps strongly with a sample of saiga antelope (*Saiga tatarica*) from the same spatio-temporal range (Fig. 5).

Discussion

Our results have implications for both the phylogenetic position and extinction of the last elasmotheriine rhinoceros, and for the pattern and causality of Late Quaternary megafaunal turnover. The deep division between *Elasmotherium sibiricum* and the extant rhinoceroses in our molecular phylogeny (Fig. 4) is strongly supportive of an ancient split between Elasmotheriinae (including *Elasmotherium*, contra refs. [4,5]) and Rhinocerotinae, in keeping with recent palaeontological evidence: the earliest fossil species referred to Elasmotheriinae are *Subhyracodon occidentalis* and *Penetrigonias dakotensis* at ca. 38 Ma[3,25], while the earliest certain representative of Rhinocerotinae is *Epiaceratherium naduongense*[26] at ca. 39-35 Ma. Our early- to mid-Eocene estimate of ~47.4 Ma for the divergence between Elasmotheriinae and Rhinocerotinae pre-dates their first fossil appearances by 8-9 Ma, with this lag likely explained by the incompleteness of taxonomic samples included in morphology-based phylogenetic analyses of Rhinocerotidae, especially regarding stem Eocene taxa[2,3].

Previously, the loss of *E. sibiricum* has been regarded as part of the 'background extinction' of large mammals that proceeded through the Early and Middle Pleistocene*.* The species was considered typical of the Singhil and Khazar faunistic complexes of Russia, broadly early and late Middle Pleistocene, respectively, with its youngest occurrences attributed to the late Middle Pleistocene, ca. 200 ka[7,8]. However, most of the remains, from locations in the Volga region, were found on river banks, with likely mixing of bones from different geological horizons. On the basis of locally associated faunas, a possible Late Pleistocene age for some of the remains had been suggested (refs. [9], and [2], p.42, but except for Smelovskaya II these specimens were also recovered *ex situ* and all radiocarbon dates on associated fauna are infinite (Supplementary Information). A radiocarbon measurement of 26,038 ± 356 BP (UBA-30522) was obtained from a partial skull of *E. sibiricum* from Kozhamzhar, Kazakhstan[27], but the context otherwise appeared Middle Pleistocene, and the laboratory indicated that the date was unreliable as collagen yield was only 0.3% after ultrafiltration[28].

Our results therefore provide reliably dated Late Pleistocene occurrences of *E. sibiricum* ranging from close to the older limit of radiocarbon dating to just before the onset of Greenland Stadial 8 (ca. 36-35 cal ka BP: ref. [29]). This places its extinction firmly within the Late Quaternary extinction event, during which approximately 40% of northern Eurasian mammal species with body weights >45 kg (megafauna) died out in the interval ca. 50-4 ka[30]. Many of these species became extinct in the Late-glacial (GI-1 & GS-1) and Holocene (MIS 1), starting from ca. 15 cal ka BP. The latest dates for *E. sibiricum* around 39-35 ka, however, form an important addition to the growing evidence for turnover in the northern Eurasian large mammal fauna before or early in the Last Glacial Maximum (LGM)[31,32]. The LGM has been variously defined, including the minimum in $\delta^{18}O$ in Greenland ice ca. 30-25 ka (Fig. 3), or the minimum sea level and maximum expansion of northern hemisphere ice sheets ca. 21 ka[33,34]. The latest dates for *E. sibiricum* are closely coincident with those for *Homo neanderthalensis* and the east Beringian stilt-legged horse *Haringtonhippus francisci*[32,35,36]. This was followed by apparent peripheral range reduction in *C. antiquitatis*[32,37], and major genetic turnover in several species including mammoth and bison[32]. The latest records of Eurasian spotted hyaena *C. crocuta* and cave bear *U. spelaeus* are at ca. 31 ka and 28-27 ka, respectively[38–41], while *Megaloceros giganteus* suffered major range collapse, recovering only in the Late-glacial (GI-1)[42]. The available dates for *E. sibiricum* strongly corroborate this pre-LGM phase of faunal turnover. There are many fossil localities within the sampled geographical area that have produced later dates for other megafauna[20,43], so the absence of *Elasmotherium* is unlikely to be due to lack of suitable assemblages.

The inferred timing of these events falls during a period of pronounced climate and environmental change, the series of Greenland Stadials and Interstadials that characterised Marine Isotope Stage 3[32]. The start of the dated faunal events, including the last appearance of *E. sibiricum*, are approximately coincident with GS-8 and Heinrich stadial 4, a major episode of ice rafting into the North Atlantic[44]. Plant, insect and lithostratigraphic proxies from across northern Eurasia corroborate a sustained shift to cold tundra-steppe beginning around 35 ka ^{14}C BP (equivalent to 40-38 ka), with the breakup of grass/herb-dominated vegetation cover[45]. These changes are a potential contributor to the turnover and extinction of large mammals in the interval preceding the LGM, but further data are required to examine their regional effects in areas such as the central Asian range of *E. sibiricum.*

The extinction of *Elasmotherium* may also have been linked to its high degree of specialisation, including extreme dietary adaptations[7]. Among other rhinoceros species, morphological and tooth-wear data show that *S. kirchbergensis* and *S. hemitoechus* were browse- and graze-dominated mixed-feeders, respectively, while *C. antiquitatis* was a grazer[46–49]. In *E. sibiricum* the obtuse angle between the plane of the occiput and the palate indicates that the head was carried lower even than in the woolly rhinoceros and the living white rhino[50,51], an extreme adaptation to feeding close to the ground. The hypsodont, rootless, permanently-growing cheek teeth, with highly convoluted enamel, imply hypergrazing adaptation and/or the consumption of substantial quantities of dust or grit. Our stable isotope analyses of *E. sibiricum* also show values clearly differing from those of other rhinoceros species (Fig. 5). Pollen, plant macrofossil and faunal data suggest that during MIS 3, the areas inhabited by *E. sibiricum* included open steppe habitats in the southern Trans-Urals, while in other areas forest-steppe landscapes with extensive grassy areas were present[52]. High $\delta^{13}C$ and $\delta^{15}N$ values, seen in *E. sibiricum*, are typical for mammals inhabiting a dry steppe or desert biotope[53]. The $\delta^{13}C$ values of *E. sibiricum* may also have been influenced by the consumption of Chenopodiaceae (C4 photosynthesisers), as in modern saiga antelope *Saiga tatarica*[54], and/or to the pulling up and consumption of roots (as suggested for *E. sibiricum*[7]), since non-photosynthetic plant parts tend to be elevated in $\delta^{13}C$ (ref. [55]).

Previous stable isotope studies on mammalian herbivore species from Europe have illustrated change in ecological niches during the pre-LGM[56] and the Late glacial[57]. Both *C. antiquitatis* and *S. tatarica* survived the extinction of *E. sibiricum*, the former with an isotopic signature implying a dietary niche consistently different from that of *E. sibiricum*, the latter with a shift in its range of isotopic values. While *Saiga* samples from pre-LGM central Asia show $\delta^{13}C$ and $\delta^{15}N$ values overlapping strongly with contemporary *Elasmotherium* (Fig. 5), samples from later periods (LGM to Late-glacial Interstadial, GI-1), and those from other regions, include lower $\delta^{15}N$ values (down to +2.8 ‰), indicating dietary flexibility[54]. The implication is that both *Coelodonta* and *Saiga* could cope with the environmental change that began around 38 ka but *E. sibiricum* could not. Added to this, the persistently restricted geographical range of *Elasmotherium*, also likely linked to its specialized habitat, as well as low population size and slow reproductive rate associated with large body size[58], would have predisposed it to extinction in the face of environmental change, while the ecologically similar, but much smaller species (*S. tatarica*) survived. The extinction of *E. sibiricum* could in theory have been exacerbated by human hunting pressure, given the replacement of *H. neanderthalensis* by *H. sapiens* in Eurasia ca. 45-40 ka[59]. There is currently no record of the species' remains from any archaeological site, and the very few suggested depictions of *Elasmotherium* in Palaeolithic art (ref. [51]; ref.[2], p. 46-7) are unconvincing.

Materials and Methods

We sampled a total of 25 specimens of *E. sibiricum* from the collections of the Museum of the Institute of Plant and Animal Ecology UB RAS (Ekaterinburg), Sverdlovsk Regional History Museum (Ekaterinburg), Zoological Institute RAS (St Petersburg) and the Natural History Museum (London). Specimens were readily identified from the highly characteristic features of the skull, mandible, postcranial bones, and the hypsodont, rootless cheek teeth with their distinctive convoluted enamel. Sample provenances are detailed in the Supplementary Information.

At the Groningen Centre for Isotope Research (CIO), samples underwent standard chemical cleaning and collagen extraction following an improved version of the Longin method, as described in ref. [60] and in the Supplementary Information. In short, bone samples are decalcified over at least 24 hrs using weak HCl (4% w/vol). When CO_2 release has ceased and the fragments are soft and pliable they are rinsed thoroughly with distilled water (DW). The extract is exposed to NaOH (1%, >30 min) to eliminate humic acids, rinsed to neutrality and again treated with HCl (4% w/vol, 15 min). The raw collagen fraction is denatured to gelatin in acidified DW (pH 3) at 90 °C for 18 hrs. Dissolved gelatin is filtered through a 100 µm mesh to eliminate any remaining foreign particulates, and dried. The collagen is combusted to CO_2 using an Elemental Analyser (Isocube) connected to an Isotope Ratio Mass Spectrometer (Isoprime), providing stable isotope ratios $^{13}C/^{12}C$ and $^{15}N/^{14}N$. For ^{14}C, the CO_2 was cryogenically trapped using an automatic collection device. The routine graphitization procedure at the CIO has been operational for over 20 years[61,62], with only minor, mainly mechanical, adjustments. The $^{14}C/^{12}C$ ratio in the graphite was measured by Accelerator Mass Spectrometry[63]. At the Oxford Radiocarbon Accelerator Unit (ORAU), samples were dated using two different methods. First, samples were pre-treated following the routine procedure at the ORAU comprising decalcification in acid, a base wash, re-acidification, gelatinisation and ultrafiltration (coded '**AF**'), as described in ref. [64]. Samples that had been preserved with glues, or samples for which we did not have complete knowledge of post-excavation history, were also washed with organic solvents (acetone, methanol and chloroform) prior to AF treatment (coded '**AF***'). Samples were also re-dated using the single amino acid radiocarbon dating method optimised at ORAU[11]. This method involves separation of the underivatised amino acids using preparative High Performance Liquid Chromatography after hydrolysis of the bone collagen samples. Using this method, the amino acid hydroxyproline was isolated and then combusted, graphitised and dated by AMS. The sample C/M 12836 was prepared in duplicate as part of an internal control at the ORAU. In both laboratories the quality of the collagen (or hydroxyproline) extracted was monitored by measuring carbon and nitrogen contents (%C and %N) and the atomic ratio of carbon to nitrogen (C:N) that is acceptable in the range 2.9—3.5 in the case of collagen or ~5.0 in the case of hydroxyproline.

The ^{14}C ages were calibrated against the Northern Hemisphere calibration (IntCal13) dataset[17]. Here we used a single 'Phase' model in OxCal 4.3 (ref. [18]) coupled with a 'General' outlier model (probability = 0.05). Using Bayes theorem, the algorithms employed sample possible solutions with a probability that is the product of the prior and likelihood probabilities. Taking into account the deposition model and the actual age measurements, the posterior probability densities quantify the most likely age distributions; the 'Outlier' option was used to detect ages that fall outside the calibration model for each group, and if necessary, down-weight their contribution to the final age estimates. The 'Phase' command is a grouping model which assumes no geographic relationship between samples and that the ages represent a uniform distribution between a start and end boundary. For the model a start and end boundary is included to bracket the *Elasmotherium* 'phase'. The posterior distributions allow us to determine probability distribution functions (PDF) for the beginning and ending of the phase. Modelled ages are reported here at the 95% probability range in thousands of calendar years BP (cal ka BP; relative to AD 1950). This method has been applied to a wide range of contexts including studies on megafaunal and Neanderthal extinction[35,65], archaeological phases of occupation and ceramic development[66,67], and palaeoearthquakes[68], providing robust age estimates for the start and end of phases, often with fewer ^{14}C measurements than those reported here. In OxCal, commands or parameters are written in a CQL (Command Query Language).

The $\delta^{13}C$ and $\delta^{15}N$ values in bone collagen of a herbivorous mammal reflect the isotopic composition of the plant food and water the organism ingested during its life[69], and these are in turn related to climatic and local environmental parameters. The $\delta^{13}C$ and $\delta^{13}N$ values of terrestrial C3 plants are mainly determined by (local) environmental and biogeochemical factors, such as humidity, atmospheric CO_2 concentrations, nitrogen cycling and nutrient availability[70–72]. The stable carbon and nitrogen isotope concentrations ($\delta^{13}C$ and $\delta^{15}N$ values) of *E. sibiricum* bone collagen were measured on CO_2 by Isotope Ratio Mass Spectrometry (IRMS). Published comparative data comprised woolly rhinoceros (*Coelodonta antiquitatis*)[43], Merck's rhinoceros (*Stephanorhinus kirchbergensis*) and indeterminate *Stephanorhinus* specimens (*S. kirchbergensis* &/or narrow-nosed rhinoceros *S. hemitoechus*)[73], and saiga antelope (*Saiga tatarica*)[54]. In the case of *C. antiquitatis* and *S. tatarica* we plotted only samples from pre-LGM central Asia, for direct comparison with *E. sibiricum*.

Ancient DNA analyses were performed at the Australian Centre for Ancient DNA, University of Adelaide. DNA was extracted from six *E. sibiricum* samples using a silica-based method[74]. Sequencing libraries were then created from the DNA extracts following the protocol of ref. [75]. We enriched each of the sequencing libraries for mammalian mitochondrial DNA using a previously published set of RNA probes[76] and sequenced them on an Illumina MiSeq. The resulting sequencing reads were mapped to the mitochondrial genome of the extant white rhinoceros – *Ceratotherium simum* – and consensus sequences were generated for each sample using Geneious (Biomatters; http://www.geneious.com). Phylogenetic analyses were performed on these data using BEAST[77] and RAxML[78] . Additional details can be found in the Supplementary Information.

Code availability

The code used to calibrate the ^{14}C ages in OxCal is given in the Supplementary Information.

Acknowledgements

We thank Pierre-Olivier Antoine for discussion, Juha Saarinen for estimating the body mass of *Elasmotherium*, The Museum of the IPAE UB RAS and Leonid Petrov for providing bone samples for analysis, Paula Campos for help with stable isotope data, Selina Brace for initial work on ancient DNA, Willem van der Merwe for permission to reproduce his artwork in Fig. 1A, Igor Doronin for the photo in Fig. 1B, the team of the Oxford Radiocarbon Accelerator Unit for AMS dating, and Jonathan Hagstrum for an early stimulus to the study. Funding was provided by the Australian Research Council and the Natural Environment Research Council, UK (grant no. NE/G005982/1). Part of the research received funding from the European Research Council under the European Union's Seventh Framework Programme (FP7/2007-2013) - ERC grant 324139 “PalaeoChron” award to Tom Higham. The study is partly supported by the programme of the UD RAS, project number 18-4-4-3.

Author contributions

PK, TvK, AJS, AL & AC conceived the project. PK, AT & EP provided samples & contextual information. Ancient DNA work and phylogenetic analyses were performed by KJM and coordinated by AC. Radiocarbon data was obtained and analyzed by TH, TD and DC at the ORAU, and by JvdP at Groningen, while CT and TH undertook age modelling. Stable isotope analysis was performed and interpreted by MK, while CT & AJS provided context on climate and extinctions, respectively. All authors contributed to the interpretation of results and writing of the manuscript, which was co-ordinated by AL.

Additional Information

Supplementary information accompanies this paper at ……

Competing Interests: The authors declare no competing interests.

Data Availability: The four mitochondrial genome consensus sequences with coverage ≥80% and mean read-depth ≥5× are available on GenBank (MH937513-MH937516). All consensus sequences, unmapped sequencing reads, and phylogenetic analysis files associated with our ancient DNA work are available on figshare (https://figshare.com/) DOI: 10.25909/5ba34a40ba925. All the radiocarbon data generated at the ORAU and at Groningen are archived internally at the respective laboratories and are available upon request. ORAU Data is also available on the laboratory’s website with link to the paper.

References

1. Fortelius, M. *New and Old Worlds database of fossil mammals (NOW).* (University of Helsinki, 2017).
2. Antoine, P.-O. Phylogénie et Évolution des Elasmotheriina (Mammalia, Rhinocerotidae). *Mem. du Museum Natl. d'Histoire Nat.* **188,** 1–359 (2002).
3. Becker, D., Antoine, P. O. & Maridet, O. A new genus of rhinocerotidae (Mammalia, Perissodactyla) from the Oligocene of Europe. *J. Syst. Palaeontol.* **11,** 947–972 (2013).
4. Cerdeño, E. Cladistic analysis of the family Rhinocerotidae (Perissodactyla). *Am. Museum Novit.* **3143,** 1–25 (1995).
5. Guérin, C. & Pickford, M. Ougandatherium napakense nov. gen. nov. sp., le plus ancien Rhinocerotidae Iranotheriinae d'Afrique. *Ann. Paléontologie* **89,** 1–35 (2003).
6. Deng, T. & Zheng, M. Limb bones of Elasmotherium (Rhinocerotidae, Perissodactyla) from Nihewan (Hebei, China). *Vertebr. Pal Asiat.* **43,** 110–121 (2005).
7. Schvyreva, A. K. On the importance of the representatives of the genus Elasmotherium (Rhinocerotidae, Mammalia) in the biochronology of the Pleistocene of Eastern Europe. *Quat. Int.* **379,** 128–134 (2015).
8. Kozamkulova, B. S. Elasmotherium sibiricum und sein Verbreitungsgebiet auf dem Territorium der UdSSR. *Quartärpaläontologie* **4,** 85–91 (1981).
9. Kosintsev, P. A. Elasmotherium sibericum Fisher (1808). New data on the period of existence and geographic range. in *The Quaternary of the Urals: Global Trends and Pan-European Quaternary Records* 67–68 (UrFU, 2014).
10. Lister, A. M. & Stuart, A. J. Extinction chronology of the woolly rhinoceros Coelodonta antiquitatis: Reply to Kuzmin. *Quaternary Science Reviews* **62,** 144–146 (2013).
11. Devièse, T., Comeskey, D., McCullagh, J., Bronk Ramsey, C. & Higham, T. New protocol for compound-specific radiocarbon analysis of archaeological bones. *Rapid Commun. Mass Spectrom.* **32,** 373–379 (2018).
12. Bourrillon, R. *et al.* A new Aurignacian engraving from Abri Blanchard, France: Implications for understanding Aurignacian graphic expression in Western and Central Europe. *Quat. Int.* (2017). doi:10.1016/j.quaint.2016.09.063
13. Devièse, T. *et al.* Direct dating of Neanderthal remains from the site of Vindija Cave and implications for the Middle to Upper Paleolithic transition. *Proc. Natl. Acad. Sci. U. S. A.* **114,** 10606–10611 (2017).
14. Reynolds, N., Dinnis, R., Bessudnov, A. A., Devièse, T. & Higham, T. The Kostënki 18 child burial and the cultural and funerary landscape of Mid Upper Palaeolithic European Russia. *Antiquity* **91,** 1435–1450 (2017).
15. Devièse, T. et al. Increasing accuracy for the radiocarbon dating of sites occupied by the first Americans. *Quat. Sci. Rev.* **198,** 171–180 (2018).
16. Becerra-Valdivia, L. et al. Reassessing the chronology of the archaeological site of Anzick. *Proc. Natl. Acad. Sci.* (2018). doi:10.1073/pnas.1803624115
17. Reimer, P. J. *et al.* IntCal13 and Marine13 Radiocarbon Age Calibration Curves 0–50,000 Years cal BP. *Radiocarbon* **55,** 1869–1887 (2013).
18. Bronk Ramsey, C. Recent and Planned Developments of the Program OxCal. *Radiocarbon* **55,** 720–730 (2013).
19. Bronk Ramsey, C. Bayesian analysis of radiocarbon dates. *Radiocarbon* **51,** 337–360 (2009).
20. Kosintsev, P. A. *(Ed.) Ural and Siberia faunas at Pleistocene and Holocene Times*. (Russian Academy of Science, Urals Division. Institute of Plant and Animal Ecology, 2005).
21. Vasil'ev, S. A. Faunal exploitation, subsistence practices and Pleistocene extinctions in Palaeolithic Siberia. *Deinsea* **9,** 513–556 (2003).

22. Price, S. A. & Bininda-Emonds, O. R. P. A comprehensive phylogeny of extant horses, rhinos and tapirs (Perissodactyla) through data combination. *Zoosystematics Evol.* **85,** 277–292 (2009).

23. Steiner, C. C. & Ryder, O. A. Molecular phylogeny and evolution of the Perissodactyla. *Zool. J. Linn. Soc.* **163,** 1289–1303 (2011).

24. Meredith, R. W. *et al.* Impacts of the cretaceous terrestrial revolution and KPg extinction on mammal diversification. *Science* **334,** 521–524 (2011).

25. Heissig, K. The American genus Penetrigonias Tanner & Martin, 1976 (Mammalia: Rhinocerotidae) as a stem group elasmothere and ancestor of Menoceras Troxell, 1921. *Zitteliana* **A 52,** 79–95 (2012).

26. Boehme, M. *et al.* Na Duong (northern Vietnam) – an exceptional window into Eocene ecosystems from Southeast Asia. *Zitteliana* **A 53,** 120–167 (2013).

27. Shpansky, A. V., Ilyina, S. A. & Aliyasova, V. N. The Quaternary mammals from Kozhamzhar locality (Pavlodar Region, Kazakhstan). *Am. J. Appl. Sci.* **13,** 189–199 (2016).

28. Reimer, P. J. & Svyatko, S. V. Comment on Shpansky et al. 2016, The Quaternary mammals from Kozhamzhar locality (Pavlodar region, Kazakhstan). *Am. J. Appl. Sci.* **13,** 477–478 (2016).

29. Rasmussen, S. O. *et al.* A stratigraphic framework for abrupt climatic changes during the Last Glacial period based on three synchronized Greenland ice-core records: refining and extending the INTIMATE event stratigraphy. *Quat. Sci. Rev.* **106,** 14–28 (2014).

30. Stuart, A. J. Late Quaternary megafaunal extinctions on the continents: A short review. *Geol. J.* **50,** 338–363 (2015).

31. Stuart, A. J. & Lister, A. M. Patterns of Late Quaternary megafaunal extinctions in Europe and northern Asia. *Cour. Forschungsinstitut Senckenb.* **259,** 289–299 (2007).

32. Cooper, A. *et al.* Abrupt warming events drove Late Pleistocene Holarctic megafaunal turnover. *Science* **349,** 602–606 (2015).

33. Hughes, P. D. & Gibbard, P. L. A stratigraphical basis for the Last Glacial Maximum (LGM). *Quat. Int.* **383,** 174–185 (2015).

34. Monegato, G., Scardia, G., Hajdas, I., Rizzini, F. & Piccin, A. The Alpine LGM in the boreal ice-sheets game. *Sci. Rep.* **7,** 2078 (2017).

35. Higham, T. *et al.* The timing and spatiotemporal patterning of Neanderthal disappearance. *Nature* **512,** 306–309 (2014).

36. Heintzman, P. D. *et al.* A new genus of horse from pleistocene North America. *Elife* (2017). doi:10.7554/eLife.29944

37. Stuart, A. J. & Lister, A. M. Extinction chronology of the woolly rhinoceros Coelodonta antiquitatis in the context of late Quaternary megafaunal extinctions in northern Eurasia. *Quaternary Science Reviews* **51,** 1–17 (2012).

38. Stuart, A. J. & Lister, A. M. New radiocarbon evidence on the extirpation of the spotted hyaena (Crocuta crocuta (Erxl.)) in northern Eurasia. *Quat. Sci. Rev.* **96,** 108–116 (2014).

39. Dinnis, R., Pate, A. & Reynolds, N. Mid-to-late Marine Isotope Stage 3 mammal faunas of Britain: a new look. *Proc. Geol. Assoc.* **127,** 435–444 (2016).

40. Pacher, M. & Stuart, A. J. Extinction chronology and palaeobiology of the cave bear (Ursus spelaeus). *Boreas* **38,** 189–206 (2009).

41. Bocherens, H. *et al.* The last of its kind? Radiocarbon, ancient DNA and stable isotope evidence from a late cave bear (Ursus spelaeus ROSENMÜLLER, 1794) from Rochedane (France). *Quat. Int.* **339–340,** 179–188 (2014).

42. Stuart, A. J., Kosintsev, P. A., Higham, T. & Lister, A. M. Pleistocene to Holocene extinction dynamics in giant deer and woolly mammoth. *Nature* **431,** 684–689 (2004).

43. Stuart, A. J. & Lister, A. M. Extinction chronology of the woolly rhinoceros Coelodonta antiquitatis in the context of late Quaternary megafaunal extinctions in northern Eurasia. *Quaternary Science Reviews* **51,** 1–17 (2012).

44. Guillevic, M. *et al.* Evidence for a three-phase sequence during heinrich stadial 4 using a

multiproxy approach based on Greenland ice core records. *Clim. Past* **10,** 2115–2133 (2014).

45. Hubberten, H. W. *et al.* The periglacial climate and environment in northern Eurasia during the Last Glaciation. *Quat. Sci. Rev.* **23,** 1333–1357 (2004).
46. Boeskorov, G. G. *et al.* Woolly rhino discovery in the lower Kolyma River. *Quat. Sci. Rev.* **30,** 2262–2272 (2011).
47. Rivals, F. & Lister, A. M. Dietary flexibility and niche partitioning of large herbivores through the Pleistocene of Britain. *Quat. Sci. Rev.* **146,** 116–133 (2016).
48. Saarinen, J., Eronen, J., Fortelius, M., Seppä, H. & Lister, A. M. Patterns of diet and body mass of large ungulates from the Pleistocene of Western Europe, and their relation to vegetation. *Palaeontol. Electron.* **19,** 1–58 (2016).
49. Pushkina, D., Bocherens, H. & Ziegler, R. Unexpected palaeoecological features of the Middle and Late Pleistocene large herbivores in southwestern Germany revealed by stable isotopic abundances in tooth enamel. *Quat. Int.* **339–340,** 164–178 (2014).
50. Zeuner, F. E. New reconstructions of the woolly rhinoceros and Merck's rhinoceros. *Proc. Linn. Soc. London* **156,** 183–195 (1945).
51. Zhegallo, V. *et al.* On the fossil rhinoceros Elasmotherium (including the collections of the Russian Academy of Sciences). *Cranium* **22,** 17–40 (2005).
52. Grichuk, V. P. Vegetation in the Late Pleistocene. in *Dynamics of terrestrial landscape components and inner marine basins of Northern Eurasia during the last 130,000 years* (ed. Velichko, A. A.) 64–88 (GEOS Publishers, 2002).
53. Bocherens, H. Isotopic biogeochemistry and the paleoecology of the mammoth steppe fauna. *Deinsea* **9,** 57–76 (2003).
54. Jürgensen, J. *et al.* Diet and habitat of the saiga antelope during the late Quaternary using stable carbon and nitrogen isotope ratios. *Quat. Sci. Rev.* **160,** 150–161 (2017).
55. Badeck, F.-W., Tcherkez, G., Nogués, S., Piel, C. & Ghashghaie, J. Post-photosynthetic fractionation of stable carbon isotopes between plant organs—a widespread phenomenon. *Rapid Commun. Mass Spectrom.* **19,** 1381–1391 (2005).
56. Drucker, G. *et al.* Tracking possible decline of woolly mammoth during the Gravettian in Dordogne (France) and the Ach Valley (Germany) using multi-isotope tracking (13C, 14C, 15N, 34S, 18O). *Quat. Int.* **360,** 304–317 (2015).
57. Drucker, D. G., Bocherens, H. & Péan, S. Isotopes stables (13C,15N) du collagène des mammouths de Mezhyrich (Epigravettien, Ukraine): Implications paléoécologiques. *Anthropol.* **118,** 504–517 (2014).
58. Johnson, C. N. Determinants of loss of mammal species during the Late Quaternary ' megafauna ' extinctions : life history and ecology , but not body size. *Proc. R. Soc. B* **269,** 2221–2227 (2009).
59. Higham, T.; Douka, K.; Wood, R.; Bronk Ramsey, C.; Brock, F. The timing and spatiotemporal patterning of Neanderthal disappearance. *Nature* **512,** 306–309 (2014).
60. Mook, W. G. & Streurman, H. J. Physical and chemical aspects of radiocarbon dating. in *14C and Archaeology* (ed. Mook, W.G., Waterbolk, H. T.) 31–55 (1983).
61. Wijma, S., Aerts, A. T., van der Plicht, J. & Zondervan, A. The Groningen AMS facility. *Nucl. Instruments Methods Phys. Res. Sect. B Beam Interact. with Mater. Atoms* **113,** 465–469 (1996).
62. Aerts-Bijma, A. T., Meijer, H. A. J. & van der Plicht, J. AMS sample handling in Groningen. *Nucl. Instruments Methods Phys. Res. Sect. B Beam Interact. with Mater. Atoms* **123,** 221–225 (1997).
63. Van Der Plicht, J., Wijma, S., Aerts, A. T., Pertuisot, M. H. & Meijer, H. A. J. Status report: The Groningen AMS facility. *Nucl. Instruments Methods Phys. Res. Sect. B Beam Interact. with Mater. Atoms* **172,** 58–65 (2000).
64. Brock, F., Higham, T., Ditchfield, P. & Ramsey, C. B. Current pretreatment methods for ams radiocarbon dating at the oxford radiocarbon accelerator unit (ORAU). *Radiocarbon* **52,** 103–

112 (2010).

65. Metcalf, J. L. *et al.* Synergistic roles of climate warming and human occupation in Patagonian megafaunal extinctions during the Last Deglaciation. *Sci. Adv.* **2,** e1501682–e1501682 (2016).
66. Turney, C. S. M., Jones, R. T., Thomas, Z. A., Palmer, J. G. & Brown, D. Extreme wet conditions coincident with Bronze Age abandonment of upland areas in Britain. *Anthropocene* **13,** 69–79 (2016).
67. Finkelstein, I. & Piasetzky, E. Radiocarbon dating the Iron Age in the Levant: A Bayesian model for six ceramic phases and six transitions. *Antiquity* **84,** 374–385 (2010).
68. Lienkaemper, J. J. & Ramsey, C. B. OxCal: Versatile Tool for Developing Paleoearthquake Chronologies--A Primer. *Seismol. Res. Lett.* **80,** 431–434 (2009).
69. Kohn, M. J. You are what you eat. *Science* **283,** 335–6 (1999).
70. Szpak, P. Complexities of nitrogen isotope biogeochemistry in plant-soil systems: implications for the study of ancient agricultural and animal management practices. *Front. Plant Sci.* **5,** 288 (2014).
71. Nadelhoffer, K. *et al.* 15N natural abundances and N use by tundra plants. *Oecologia* **107,** 386–394 (1996).
72. Michener, R. & Lajtha, K. *Stable Isotopes in Ecology and Environmental Science*. (Blackwell, 2007).
73. Kuitems, M. *et al.* Carbon and nitrogen stable isotopes of well-preserved, Middle Pleistocene bone collagen from Schöningen (Germany) and their palaeoecological implications. *J. Hum. Evol.* **89,** 105–113 (2015).
74. Brotherton, P. *et al.* Neolithic mitochondrial haplogroup H genomes and the genetic origins of Europeans. *Nat. Commun.* **4,** 1764 (2013).
75. Meyer, M. & Kircher, M. Illumina sequencing library preparation for highly multiplexed target capture and sequencing. *Cold Spring Harb. Protoc.* **5,** pdb.prot5448 (2010).
76. Mitchell, K. J. *et al.* Ancient mitochondrial DNA reveals convergent evolution of giant short-faced bears (Tremarctinae) in North and South America. *Biol. Lett.* **12,** 20160062 (2016).
77. Drummond, A. J. & Rambaut, A. BEAST: Bayesian evolutionary analysis by sampling trees. *BMC Evol. Biol.* **7,** 214 (2007).
78. Stamatakis, A. RAxML version 8: A tool for phylogenetic analysis and post-analysis of large phylogenies. *Bioinformatics* **30,** 1312–1313 (2014).
79. Van der Merwe, W. S. Elasmotherium caucasicum. *Deviant Art* (2018). Available at: https://www.deviantart.com/willemsvdmerwe/.
80. Rohling, E. J. *et al.* New constraints on the timing of sea level fluctuations during early to middle marine isotope stage 3. *Paleoceanography* **23,** n/a-n/a (2008).
81. Ehlers, J. & Gibbard, P. L. Quaternary glaciations: extent and chronology. Parts 1-3. in *Developments in Quaternary Science 2* (Elsevier).
82. Andersen, K. K. *et al.* The Greenland Ice Core Chronology 2005, 15–42 ka. Part 1: constructing the time scale. *Quat. Sci. Rev.* **25,** 3246–3257 (2006).

Figure Captions

Figure 1: (A) Artist's impression of *Elasmotherium* in life (from ref[79]). (B) Mounted skeleton of *E. sibiricum* from Gaevskaja Village near Stavropol, south-west Russia, on display in the Stavropol Museum (length of skeleton approximately 410 cm, height 250 cm; photo by Dr. Igor Doronin).

Figure 2: Map of distribution and samples analysed. Dashed line: total range of specimens referred to *E. sibiricum*[7,8]. Red circles: samples producing radiocarbon and stable isotope data. Blue circles: samples producing radiocarbon, stable isotope and DNA sequence data. Black circles: no collagen. Note: there are fewer mapped points than actual samples analysed, because of multiple samples

from some localities. Map shows ice sheets (grey shading) and bathymetry for MIS 3 (from refs. [43,80,81]).

Figure 3: Plot of calibrated ages for *E. sibiricum* (calibrated with IntCal13 in OxCal v4.3). Median ages are represented as vertical black lines with 95.4% confidence limits as associated grey bars (HYP dates in darker grey). The blue bar represents our estimate (95.4% posterior distribution) for the last appearance of *Elasmotherium* as derived from our Phase model. The NGRIP $\delta^{18}O$ Greenland ice core record is shown as a proxy for temperature (more positive values representing warmer temperatures). The maximum counting error reported for the Greenland timescale (GICC05) is considered to approximate the 2σ uncertainty[82]; for the start of S5 (GS-5.1), this is 1008 years[29]. Greenland stadials (S1 to S8) and interstadials (I1 to I8) are indicated.

Figure 4: Maximum clade credibility tree of rhinoceroses and selected outgroup perissodactyls resulting from our time-calibrated BEAST analyses. Scale is in millions of years before the present. Node heights represent mean age estimates, while node bars represent 95% Highest Posterior Densities (HPDs). Branch support values (BEAST posterior probability / maximum likelihood bootstrap %) are presented in black text for nodes that received less than unequivocal support (i.e. 1.0 / 100).

Figure 5: Stable carbon ($\delta^{13}C$) and nitrogen ($\delta^{15}N$) values of *Elasmotherium sibiricum* samples, compared to those of Late Pleistocene woolly rhinoceros (*Coelodonta antiquitatis*[43]), Middle Pleistocene Merck's rhinoceros (*Stephanorhinus kirchbergensis*[73]) and/or narrow-nosed rhinoceros (*Stephanorhinus hemitoechus*[73]) and Late Pleistocene saiga antelope (*Saiga tatarica*[54]). *Coelodonta* and *Saiga* data are restricted to the spatio-temporal extent of our *E. sibiricum* samples.

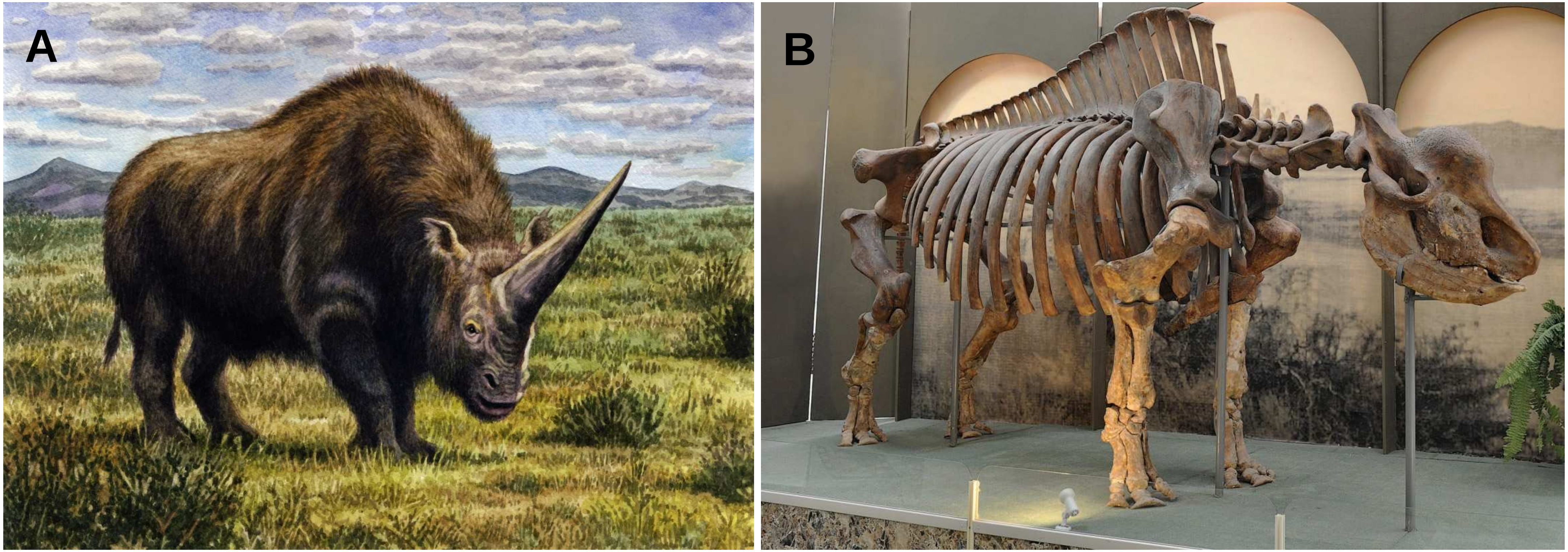
A
B

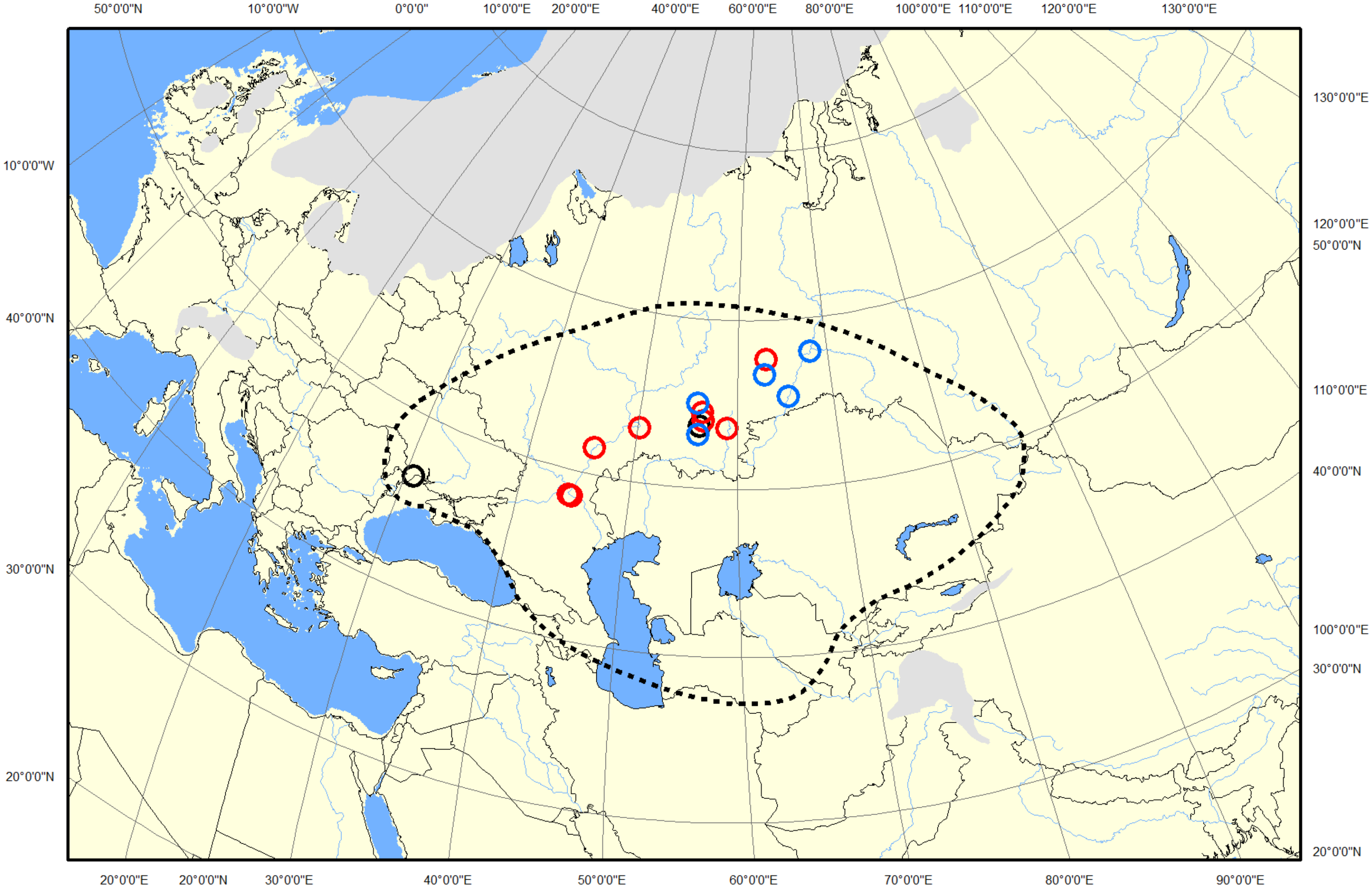
50°0'0"N
10°0'0"W
0°0'0"
10°0'0"E
20°0'0"E
40°0'0"E
60°0'0"E
80°0'0"E
100°0'0"E
110°0'0"E
120°0'0"E
130°0'0"E
10°0'0"W
40°0'0"N
30°0'0"N
20°0'0"N
130°0'0"E
120°0'0"E
50°0'0"N
110°0'0"E
40°0'0"N
100°0'0"E
30°0'0"N
20°0'0"N
20°0'0"E
20°0'0"N
30°0'0"E
40°0'0"E
50°0'0"E
60°0'0"E
70°0'0"E
80°0'0"E
90°0'0"E

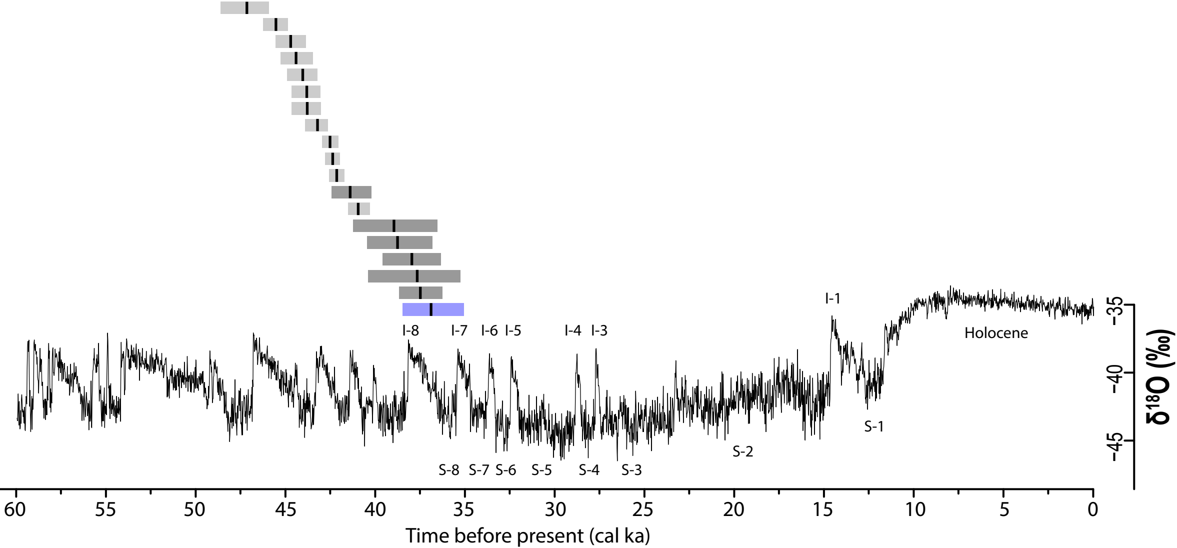
I-1
I-8
I-7
I-6
I-5
I-4
I-3
Holocene
S-1
S-2
S-8
S-7
S-6
S-5
S-4
S-3
−35
−40
−45
δ¹⁸O (‰)
60
55
50
45
40
35
30
25
20
15
10
5
0
Time before present (cal ka)

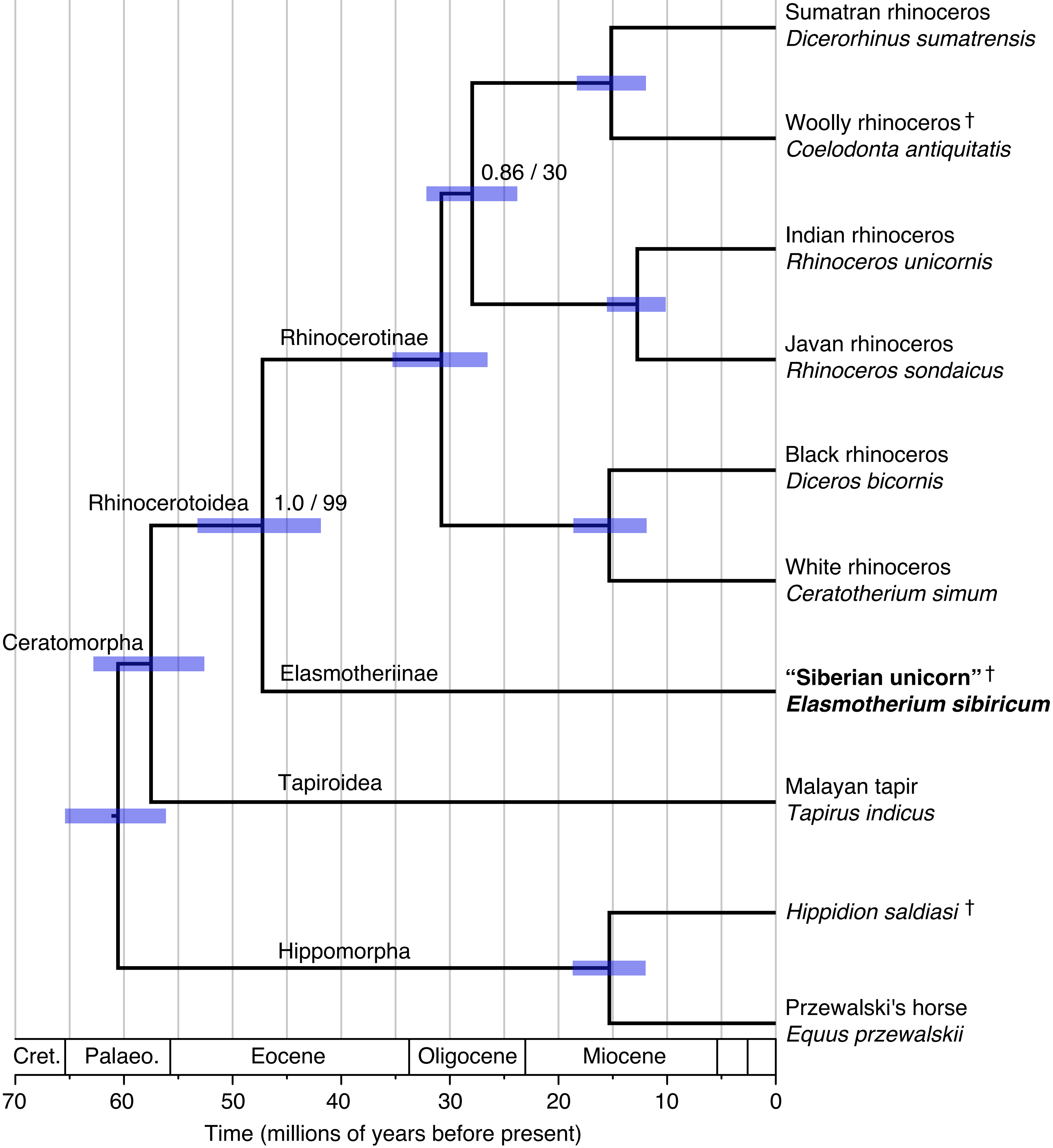
Sumatran rhinoceros
Dicerorhinus sumatrensis
Woolly rhinoceros †
Coelodonta antiquitatis
0.86 / 30
Indian rhinoceros
Rhinoceros unicornis
Rhinocerotinae
Javan rhinoceros
Rhinoceros sondaicus
Black rhinoceros
Diceros bicornis
Rhinocerotoidea
1.0 / 99
White rhinoceros
Ceratotherium simum
Ceratomorpha
Elasmotheriinae
"Siberian unicorn" †
Elasmotherium sibiricum
Tapiroidea
Malayan tapir
Tapirus indicus
Hippidion saldiasi †
Hippomorpha
Przewalski's horse
Equus przewalskii
Cret.
Palaeo.
Eocene
Oligocene
Miocene
70
60
50
40
30
20
10
0
Time (millions of years before present)

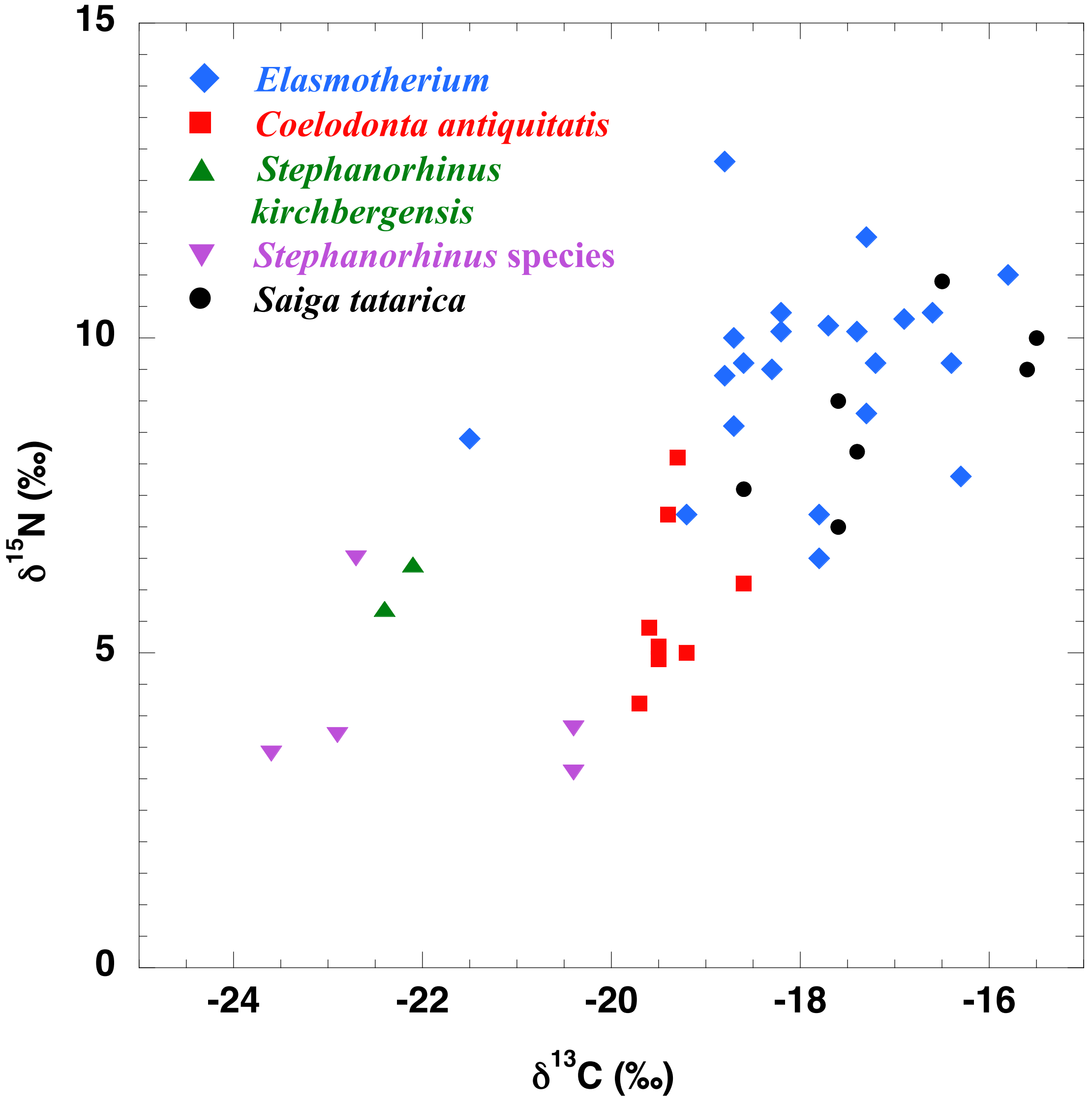
15
10
5
0
-24
-22
-20
-18
-16
δ15N (‰)
δ13C (‰)
Elasmotherium
Coelodonta antiquitatis
Stephanorhinus kirchbergensis
Stephanorhinus species
Saiga tatarica